Journal of the Brazilian Society of Mechanical Sciences and Engineering (2023) 45:119
https://doi.org/10.1007/s40430-023-04025-z

TECHNICAL PAPER

Analysis and compensation of positioning errors of robotic systems by an interactive method

Sid-Ahmed Dahmane[1] · Abdelkader Slimane[2,3] · Mohammed Chaib[4] · Mohammed Kadem[5] · Larbi Nehari[5] · Sid-Ahmed Slimane[2,6] · Abdelwahab Azzedine[1]

Received: 4 July 2022 / Accepted: 4 January 2023 / Published online: 1 February 2023

Abstract
In this work, we study the parameters influencing the positioning and rotation accuracy of industrial robot manipulators. From the Denavit–Hartenberg model (standard or modified DH) and the generalized transformation matrix, position and rotation is carried out in the general case and then applied to the Puma 560 robot. To illustrate this work, a program is developed using the symbolic calculation tools of this language was developed for the calculation of the robot's precision for given absolute uncertainties. Calculate errors positions in each case. Once the error values have been calculated and compared with other authors, we use these results to determine the influence of each parameter on the errors positions, and to see which is the most influential and secondly proposed a model that represents the analytical part of this method and gives a confidence interval of each parameter.

Keywords Accuracy · Denavit–Hartenberg parameters (D–H) · Static parameters · Robot manipulator · DOE analysis

1 Introduction

Recent applications of robotics in the medical field (computer-assisted surgical operations, remote control) require precision in the execution of increasingly advanced maneuvers, particularly in heavy procedures (neurosurgery, cardiac surgery, etc.). Performance specifications in robotic applications are becoming more and more severe, and increasingly accurate robots are required. However, one must first define precision for robotic systems. Several aspects are to be considered: material aspect (assembly, choice of materials),—control aspect (control strategy, quality of the corrector),—metrological aspect (sensor resolution, accuracy of measurement, tolerance of components robot) [1–4].

To improve accuracy (i.e., reduce laying errors), it is necessary to evaluate the "true" values of the geometric parameters of the robot and to insert them later into the equations of inverse geometric model (MGI). This operation is called the geometric calibration (EG) of the robots. Since it is not always possible to perform direct measurements to obtain the actual values of the parameters, the calibration approaches proposed in the literature are based mainly on optimization models. The values of the parameters identified by these calibration methods do not necessarily correspond to the true values of the robot parameters. Instead,

Technical Editor: Rogério Sales Gonçalves.

✉ Abdelkader Slimane
slimane.aek@hotmail.com

[1] Laboratory of Structures and Solids Mechanics (LMSS), University Djilali Liabès of Sidi-Bel-Abbes, 22000 Sidi Bel Abbes, Algeria

[2] Laboratoire de Mécanique Appliquée, Département de Génie Mécanique, Université des Sciences et de la Technologie d'Oran Mohamed Boudiaf, USTO-MB, BP 1505, El M'naouer, 31000 Oran, Algeria

[3] Laboratory of Materials and Reactive Systems (LMSR), Department of Mechanical Engineering, University of Sidi-Bel-Abbes, Bp 89, cité Ben M'hidi Sidi-Bel-Abbes, 22000 Sidi Bel Abbes, Algeria

[4] Laboratory of Intelligent Structures/DGRSDT, CTR University of Ain Temouchent, 46000 Ain Temouchent, Algeria

[5] Faculty of Electrical Engineering, University of Djillali liabes Sidi, Bel Abbes, Sidi Bel Abbes, Algeria

[6] Centre of Satellite Development (CDS), BP.: 4065, Ibn Rochd USTO, Oran, Algeria

they represent the values that satisfy the objective functions of the optimization models used in the calibration procedure.

These functions generally consist of minimizing the residual errors of poses or joint movements.

Numerous research studies have focused on the correction of the error on the accuracy and the repeatability. We also mention the work on the online correction of the positioning defects. The kinematic chain faults of an industrial robot are nevertheless, largely responsible for the degradation of positioning accuracy in static and dynamics its working volume. It depends on the play and mechanical inaccuracies [9].

The design techniques of experiments (DOE) allow designers to simultaneously determine the individual and interaction effects of many factors that could affect the output results in any design.

The DOE also provides a comprehensive overview of the interaction between design elements; therefore, it helps to transform any standard model into a robust framework. Simply, DOE helps to spot sensitive parts and sensitive factors in drawings that cause problems. Designers are then able to solve these problems and produce robust, higher-performance models before the production and manufacture of robots.

In terms of fracture, Ep error is a parameter characterizing the significant increase in position and rotation error of the robot, which is what we tried to develop in this study [11, 12], we use the method DOE to see the interaction between factors (uncertainties on DH parameters) and their influence on the response (EP position accuracy error).

A detailed organization chart that illustrates Operational process in Fig. 1.

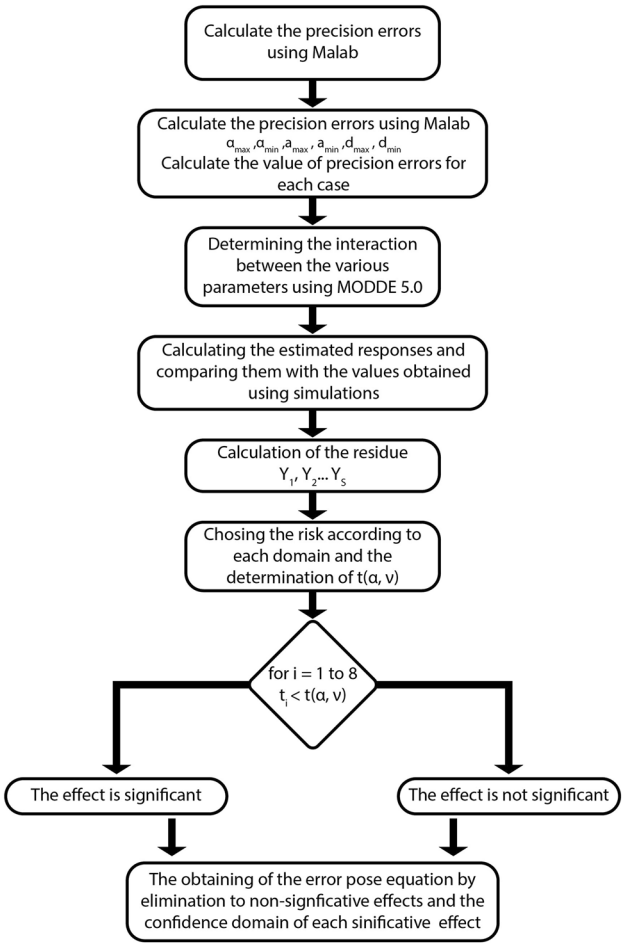

Fig. 1 Operational process

2 Literature survey

Industry today is heavily dependent on robots for a wide range of applications such as in the medical field, assembly and welding of materials. Robotic machining applications. However, improving the accuracy and repeatability of materials to meet desired process parameters is still the primary goal. For this, we have chosen to implement two methods studied separately. First of all, a calibration of the geometric parameters of its piloting model makes it possible to improve the pose precision of the robot. Then a mirror correction method [5] corrects its trajectory from the error determined between the measured and programmed trajectories (Fig. 2).

According to the sources of imprecision to be compensated, Elatta et al. (2004) present two main families of robot calibration, namely geometric calibration (GC), intended to improve the kinematic model of the robot, and non-geometric calibration, which aims to process errors of non-geometric origin. As for articular errors, they are usually included in the GC. Three levels of calibration are presented and discussed in [6]. Level 1 is joint-level calibration, Level 2 is full robot kinematic model calibration, and Level 3 is non-kinematic (non-geometric) calibration. In this work, the limits of the improvement of the precision of the robot are attributed to the limits of repeatability and precision of the robot and to the precision of the measurement system.

Sid-Ahmed et al. [7], in this work the main objective is to optimize the position and orientation error of the platform of a plane parallel manipulator robot (3RPR) using the direct geometric model. The main disadvantage of parallel manipulators is the existence of singularities within its workspace, methods are used to determine the optimal solution. The neuro-fuzzy adaptive solution is proposed in this study to find the optimal solution.

Chunche et al. [8], to achieve the stringent accuracy of some robotic applications such as robotic measurement systems, it is essential to compensate for non-geometric errors and thermal errors in addition to geometric errors. In this work article studies the effect of geometric errors, links and temperature variations on the positioning accuracy of the robot. A general methodology is developed to identify these errors simultaneously.

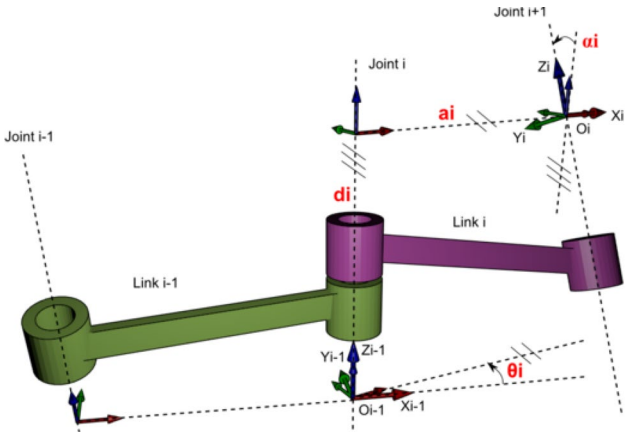

Fig. 2 The parameters D–H

A laser tracker is applied to calibrate these errors by an inverse calibration method. The geometric errors of the robot are calibrated at room temperature while the thermal errors of the robot parameters are calibrated at different temperatures as the robot warms up and cools down. Empirical thermal error models are established. These models can be integrated into the controller and used to compensate for thermal errors due to heat sources. The results show that the accuracy is improved after calibration [14–32].

This work focus on the concepts of accuracy and repeatability. A literature review on the topic is presented; the concepts of accuracy and repeatability are developed with the both contexts: homogeneous and differential transformation.

The main goal of this paper is evaluation and discussion of the DH parameters influence on the accuracy and repeatability of robots, using the techniques of experiments (DOE) methodology. To validate this study, a program is developed using the symbolic calculation tools, allowing the calculation of errors in the position of the robot starting from given uncertainties. And numerical example using published values for the PUMA 560 robot focused on the aforementioned concepts is presented and discussed.

3 Accuracy analysis

The manufacturers of industrial robots generally provide the values of the resolutions and of the repeatability measured according to the experimental protocol described in the international standard ISO 9283 [1]. It can be considered as an empirical rule that robots of large dimensions exhibit high errors of positioning repeatability.

3.1 Kinematic analysis

The kinematic structure of the manipulator robots is mathematically described by a representation Compact of the position and orientation of a given joint with respect to the articulation that precedes it. The most used is the modified Denavit–Hartenberg notation which allows to model any robotic structure [10–13]

The parameters D-H are grouped in a 4×4 matrix called a homogeneous transformation matrix ${}^{i-1}_{i}T$, which describes the position and the orientation of the reference point linked to the joint (i) relative to the reference point linked to the articulation (i-1). It is given by Eq. (1).

$$ {}^{i-1}_{i}T = \begin{bmatrix} \cos(\theta_i) & -\sin(\theta_i) & 0 & a_{i-1} \\ \sin(\theta_i)\cos(\alpha_{i-1}) & \cos(\theta_i)\cos(\alpha_{i-1}) & -\sin(\alpha_{i-1}) & -d_i\sin(\alpha_{i-1}) \\ \sin(\theta_i)\sin(\alpha_{i-1}) & \cos(\theta_i)\sin(\alpha_{i-1}) & \cos(\alpha_{i-1}) & d_i\cos(\alpha_{i-1}) \\ 0 & 0 & 0 & 1 \end{bmatrix} \tag{1} $$

In the case of the Puma 560 robot, the global homogeneous transformation matrix (from the referential linked to the tool relative to the referential linked to the robot base) is written (2–4)

$$ {}^{0}_{n}T = \prod_{i=1}^{n} {}^{i-1}_{i}T = {}^{0}_{1}T\,{}^{1}_{2}T\,{}^{2}_{3}T\ldots..{}^{n-1}_{n}T \tag{2} $$

$$ {}^{n}_{0}T = \begin{bmatrix} R_{3x3} & P_{3x1} \\ 0_{1x3} & 1 \end{bmatrix} \tag{3} $$

$R_{3x3} = f(\theta_i, \alpha_{i-1}),\quad i = 1,6$ is the orientation matrix

$P_{3x1} = f(\theta_i, a_i, d_i),$
$i = 1,6$ is the position vector of the marker linked to the terminal organ(TCP)

$$ {}^{0}_{n}T == \begin{bmatrix} r_{11} & r_{12} & r_{13} & p_x \\ r_{21} & r_{22} & r_{23} & p_y \\ r_{31} & r_{32} & r_{33} & p_z \\ 0 & 0 & 0 & 1 \end{bmatrix} \tag{4} $$

The operational coordinates calculated as follows:

$$ P = \begin{bmatrix} p_x = \cos(\theta_1)\left[a_2\cos(\theta_2) + a_3\cos(\theta_2+\theta_3) - d_4\sin(\theta_2+\theta_3)\right] - d_3\sin(\theta_1) \\ p_y = \sin(\theta_1)\left[a_2\cos(\theta_2) + a_3\cos(\theta_2+\theta_3) - d_4\sin(\theta_2+\theta_3)\right] + d_3\cos(\theta_1) \\ p_z = -a_3\sin(\theta_2+\theta_3) - a_2\sin(\theta_2) - d_4\cos(\theta_2+\theta_3) \end{bmatrix} \tag{5} $$

3.2 Analysis of errors

Only the resulting error on the position of the tool-related mark will be considered, and subsequent analysis of the error occurring on the rotation matrix will be carried out. The precision and repeatability of a manipulator can be deduced from (1) by substituting the values of the parameters D-H given on Table 1 and the values of the angles of the corresponding joints. However, the actual positions of the robot are not only a function of the D-H parameters, but also of their possible uncertainties. Which come either from the construction, mounting tolerances or limitations of devices such as position sensors (resolution of optical encoders). By limiting ourselves to the first-order errors which will be denoted by, the theory of differential transformations applied to matrix functions, allows us to write, if we put:

$$T_i = T_i(\alpha, a, \theta, d) \tag{6}$$

$$T_i = T_i \pm \Delta T_i \tag{7}$$

$$\Delta T_i = \frac{\partial T_i}{\partial \alpha}\Delta\alpha_i + \frac{\partial T_i}{\partial a}\Delta a_i + \frac{\partial T_i}{\partial \theta}\Delta\theta_i + \frac{\partial T_i}{\partial d}\Delta d_i \tag{8}$$

$$T = T_i \pm (\frac{\partial T_i}{\partial \alpha}\Delta\alpha_i + \frac{\partial T_i}{\partial a}\Delta a_i + \frac{\partial T_i}{\partial \theta}\Delta\theta_i + \frac{\partial T_i}{\partial d}\Delta d_i) \tag{9}$$

It is then possible to deduce the generalized matrix defining the orientation and the current positions of the mark of the tool with respect to the base mark either in analytical form or in digital form provided that the error associated with each parameter is known. Generally these values are not provided by the robot constructor, however, a reasonable estimate of the maximum tolerance corresponding to the structural parameters (α, a, d) and the angular error related to the tolerance of the angular position sensor can be given.

3.3 Accuracy calculation

The boundaries of the current position vector $[P_{cx}, P_{cy}, P_{cz}]$ of the tool-related coordinate system can be obtained if it is assumed that there is a deviation associated with each parameter D-H. The current position sought will then be the vector associated with the generalized transformation matrix T_c.The resulting error e_i corresponds to the difference between the current position and the theoretical position for the three spatial coordinates (10)

$$e_i = P_{ci} - P_{ti}, \quad i = \{x, y, z\} \tag{10}$$

The global error will be defined as the Euclidean norm of the maximum errors committed on the three spatial coordinates:

$$e_g = \sqrt{\max(e_x)^2 + \max(e_y)^2 + \max(e_z)^2} \tag{11}$$

An accuracy estimate is obtained by calculating the global position error assuming that all D-H parameters are affected by errors. On the other hand, the error due to the repeatability considers only the error coming from the generalized angular coordinates (case of the Puma 560).This is because once the robot is assembled, the only changes that can occur are the position instructions (angular rotations of the joints). All other parameters are static and are not likely to vary during an operating sequence, as long as the environmental influence quantities do not vary (temperature, pressure, humidity, load bending). Indeed once the robot is assembled, the static errors will always be present and will not influence the repeatability. Precision errors will depend on the D-H parameters and their corresponding variations. If we assume that the joints are all of the rotoid type (case of the Puma 560), we can write then:

* For precision, the error of position is written:

$$\varepsilon_P = f(\alpha_i, a_i, \theta_i, d_i, \Delta\alpha_i, \Delta a_i, \Delta\theta_i, \Delta d_i) \tag{12}$$

Precision is a function of the static (constant) parameters α_i, a_i, d_i.

Static uncertainties $\Delta\alpha_i, \Delta a_i, \Delta d_i$ are due to construction and assembly tolerances, while dynamic uncertainties $\Delta\theta_i$ arise from the resolution of the position sensors. Since the robot control scheme requires the calculation of the inverse kinematic model, only the nominal values of the static D-H parameters can be used, since the uncertainties cannot be taken into account since they are not known. This results in a systematic uncertainty of positioning which requires prior calibration.

On the other hand, repeatability is easier to predict and control, since it expresses the robot's ability to return to the same imposed position. The static quantities do not affect the repeatability, since the robot is assembled, the nominal values of the parameters D-H provided by the manufacturer can be adopted. When a position is assigned to the manipulator, all that the control system needs is the current value of the dynamic variables, in this case the

Table 1 DH of the robot Puma 560

i	α_{i-1}	a_{i-1}	θ_i	d_i
1	0	0	θ_1	*0*
2	$-\pi/2$	0	θ_2	*0*
3	0	a_2	θ_3	d_3
4	$-\pi/2$	a_3	θ_4	d_4
5	$\pi/2$	*0*	θ_5	*0*
6	$-\pi/2$	*0*	θ_6	*0*

a_2=d_4=431 mm, a_3=20.32 mm, d_3=124.46 mm

angle set points. This is the only useful information to return to the imposed position. It follows that repeatability depends only on generalized dynamic coordinates $\Delta\theta_i$.

4 Numerical example

We reproduce here below (Table 1) the values of the parameters DH of the robot Puma 560. The choice was on this Robot because of the numerous works that were devoted to him, which make it a prototype of study very documented.

After proposing a study of the modeling and the characteristics of the robot "Puma560", the next step consists in implementing the solution proposed in order to be able to simulate the behavior of the robot for the pursuit of the positions desired by the proposed control laws. In order to optimize and facilitate this essential step for a better precision and repeatability of use, we have developed a simulator which will be detailed in the following section.

5 Results obtained

We reproduce on (Table 1) the values of the modified DH parameters of the Puma 560 robot. The choice was made on this Robot because of the numerous works that have been dedicated to it, which make it a prototype of study very documented.

In Tables 2 and 3, two series of tests were carried out, one for absolute uncertainties on the static parameters corresponding to lengths (Δa, Δd), the second for absolute uncertainties on the angles.

(Δ α, Δ θ). The results of the Puma 560 robot validated in simulation are given in Figs. 4 and 5 and Tables 2 and 3.

6 Comparison of proposed approaches

From the results obtained (see Figs. 3, 4 and 5), it was found that the latter make it possible to control the position of the robot and a convergence toward the desired poses. The simulations based on the robot model are used to estimate the

Table 2 Result of the first test

N°	NDL	Δα	Δa	Δd	Δθ	Precision error	Repeatability error
01	06	0.0015	0.127	0.063	0.002	0.685261	0.172131

Table 3 Result of the second test

N°	NDL	Δα	Δa	Δd	Δθ	Precision error	Repeatability error
02	06	0.0025	0.063	0.063	0.0028	0.685811	0.234582

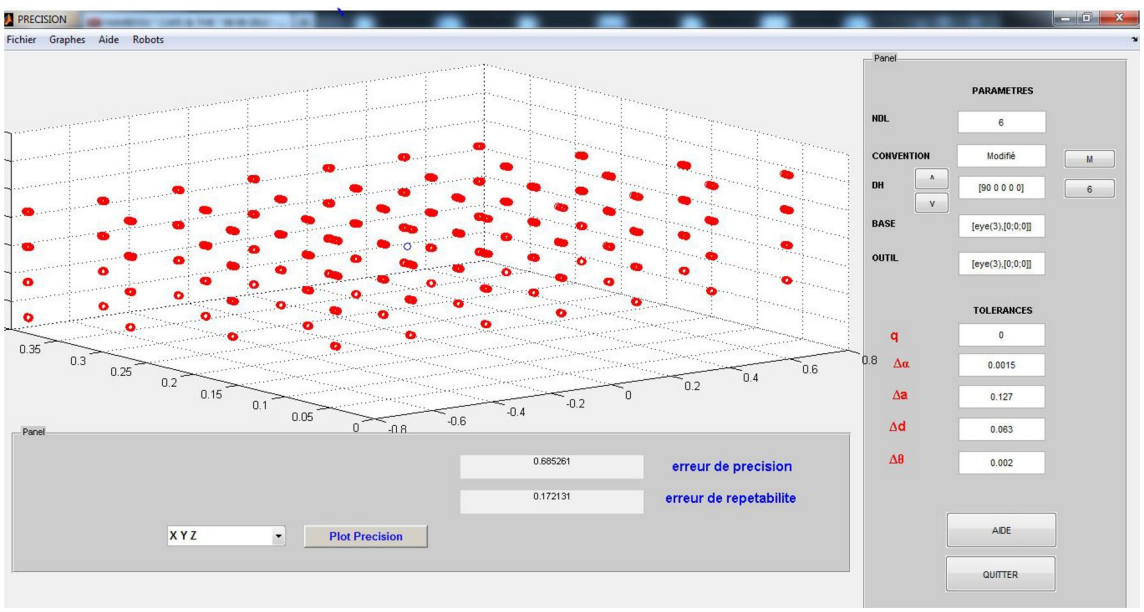

Fig. 3 Graphical interface (calculation of the precision error)

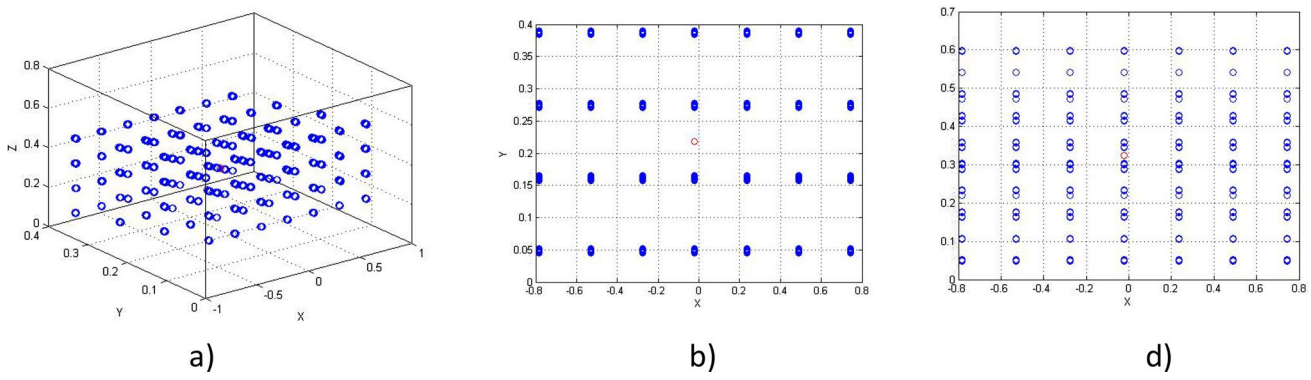

Fig. 4 Calculation of precision error of the Puma 560 robot: (**a**) Calculation of the precision error in XYZ, (**b**) Calculation of the precision error in XY, (**c**) Calculation of the error of precision in XZ

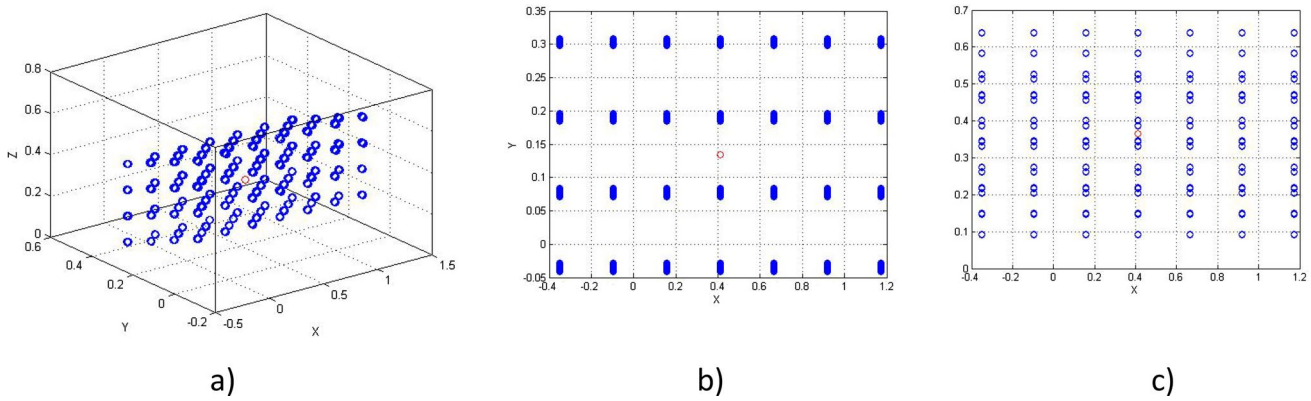

Fig. 5 Calculation of precision error of the Puma 560 robot: (**a**) Calculation of the precision error in XYZ, (**b**) Calculation of the precision error in XY, (**c**) Calculation of the error of precision in XZ

position error. From Table 1, a quantitative comparison is made by calculating the precision error along the position trajectories. According to this Table 2 and 3, the reduction of tolerance values implies better accuracy and repeatability at the desired position. If we are interested in the last case where the tolerances are considerable, a comparison can be made between the two tables starting from Table 2. The accuracy error shows good tracking of the reference positions. The same is true of the repeatability error (see Fig. 4a) The tolerance on the parameters Δa and Δd must be reduced in order to obtain a good accuracy and better follow-up of the input set points. This can be seen in Figs. 4a and 5a, whereby errors in accuracy and repeatability are reduced because of the low tolerances adopted for the Puma 560 robot.

7 Applying the experience design method

In this study, we apply an optimization method, the design method of experiments; we simulated the parameters influencing the precision of industrial robot manipulators. From the Denavit–Hardenberg model (standard or modified DH) and the generalized transformation matrix, the calculation of the precision is carried out in the general case then applied to the Puma 560 robot. To illustrate this work, a program developed and using the symbolic calculation tools of this language was developed for the calculation of the robot's precision for given absolute uncertainties. To first see the effect of each parameter α, a and d on the robot's precision error (Ep), and after seeing the most

Table 4 The parameters selected for the design of experiments method

No	Parameter	Symbol	Unit	Level	
				Low (− 1)	High (+1)
1	Angle about common normal	***α***	degree	−0.005	+0.0025
2	Length of to the common normal	***a***	mm	0.063	+0.127
3	Offset long previous z the to Common normal	***d***	mm	0.063	+0.127

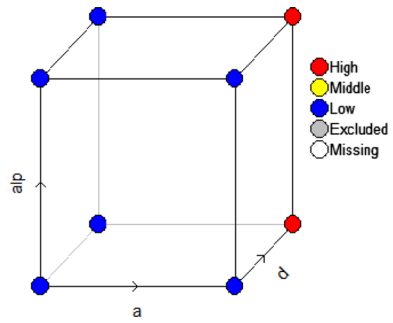

Fig. 6 Field of study

influential parameter or combination of parameters that affects the precision of our robot. To first see the effect of each parameter α, a and d on the robot's precision error (Ep), and after seeing the most influential parameter or combination of parameters that affects the precision of our robot.

7.1 Experimental matrix

In our case of three factors, the matrix of the experiments is represented by Table 4. The experimental points defining the experimental field of study are located on the vertices.

The grouping of the fields of the three factors defines the "field of study " which is the area of the experimental space chosen by the experimenter to perform the eight trials. A study, that is to say several well-defined experiments, is represented by points distributed in the study domain (Fig. 6). This way of representing an experiment by points in a logical Cartesian space is a geometric representation of the study. In this case, a plane 2^3 is associated with a mathematical model (Tables 5 and 6 and 7).

$$y = a_0 + a_1.X_1 + a_2.X_2 + a_3.X_3 + a_{12}.I_{12} + a_{13}.I_{13} + a_{23}.I_{23} \quad (13)$$

a_0: the overall averagea_1, a_2, a_3: Effect of α, a and d respectivelya_{12}: Effect of the interaction between the α and aa_{13}: Effect of the interaction between the α and da_{23}: Effect of

Table 5 Table of experiments

No Test	a (mm)≡ (X_1)	d (mm)≡ (X_2)	∝(degre)≡ (X_3)	Error precision ≡ (Y)
1	0,063	0,063	−0,005	0,007938
2	0,063	0,063	0,0025	0,007938
3	0,127	0,063	−0,005	0,0020098
4	0,127	0,063	0,0025	0,0020098
5	0,063	0,127	−0,005	0,0020098
6	0,063	0,127	0,0025	0,0020098
7	0,127	0,127	−0,005	0,032258
8	0,127	0,127	0,0025	0,032258

Table 6 Effect of factors

Effects	a_0	a_1	a_2	a_3	a_{12}	a_{13}	a_{23}
Interactions	0,0110539	4,65661e-010	0,00608	0,00608	4,80682e-010	2,103e-010	0,0090441

Table 7 Calculating predicted responses

yi	y1	y2	y3	y4	y5	y6	y7	y8
ypred	0.07938	0.07938	0.002009799	0.002009799	0.002009799	0.002009799	0.032257999	0.032257999

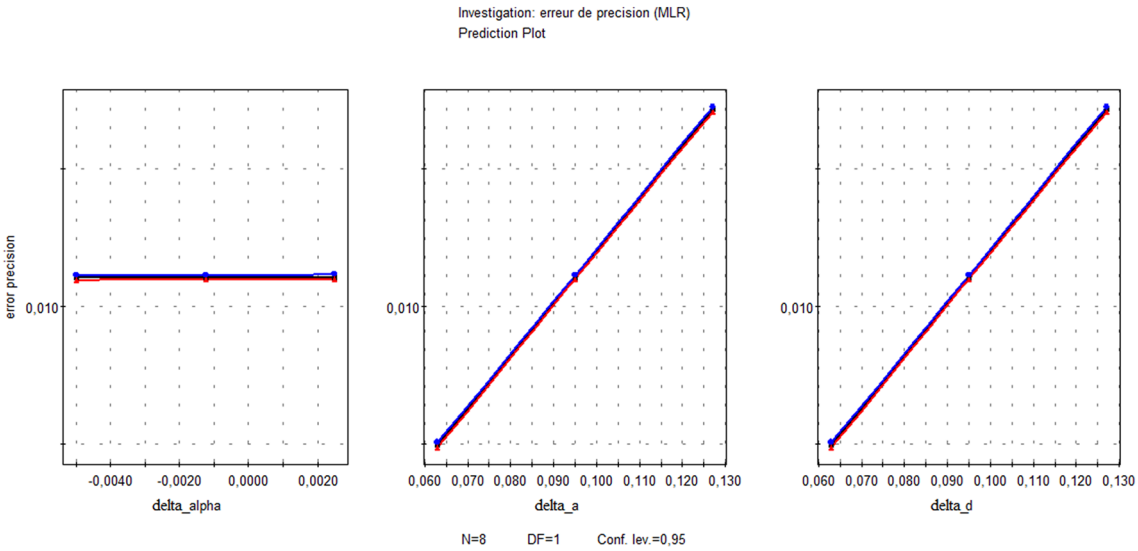

Fig. 7 Representation of the effect of the three factors

the interaction between the a and d$I_{12,}$ I_{13} and I_{23}: Interaction between the different variables.

The experimental results and the simulation presented in Fig. 7 gives us the impression that our simulation result is close to the experimental results.

7.2 Analysis with a single effect

7.2.1 Global formula of the mathematical model

$$y = 0,\ 0110539 + 4,\ 65661e - 010x_1 + 0,\ 00608x2 + 0,00608x_3 + 4,80682e - 010I_{12} + 2,103e - 010I_{13} + 0,0090441I_{23} \quad (14)$$

$$E = 0,\ 0110539 + 4,\ 65661e - 010\alpha + 0,00608\,a + 0,00608d + 4,80682e - 010I_{12} + 2,103e - 010I_{13} + 0,0090441I_{23} \quad (15)$$

7.3 Effects analysis

From Fig. 7, we will represent the effect of each factor [α (X1), a (X2) and d (X3)] on the response (precision error Ep).

In this section we will try to analyze the effect of the three main factors. First, the first remark is the direction of the three straight lines, this means that the transition from low to high for all factors causes precision (upward) and linear errors. It can be observed that for the value of Δd of 0.100 mm, the precision error is equal to 0.015 mm (c). The behavior is the same for the second effect (a) figure (b).The second remark concerning the slope of the straight line corresponding to the first factor, which is practically horizontal, indicates that this factor has no influence on the error (not significant).

7.4 Interaction effect for two factors

It is possible to create interaction graphs, when we select a two factor interaction, the predicted change in the response

In this case (Fig. 8a), it is a question of leaving the Δd constant and of varying the robot's Δα and the Δa to illustrate the precision error. First, we notice that increasing the robot's Δα and Δa at the same time increases the precision error. The horizontal analysis of Fig. 8b shows that for Δα of 0.075° we go from an error of 0.005 for Δa of the robot of 0.08 mm to an error of 0.0086 for a value of 0.12 mm. Going to Δα of 0.11°, the precision error goes from 0.0147 for a 0.11 mm to an error of 0.0147 for Δa of 0.11 mm. In other words, increasing one of the two factors or both at the same time causes an increase in the error.

It is therefore a matter of varying the value Δα of the robot in the range from −0.005° to 0.002° as well as Δd 0.07 mm to 0.12 mm, the value Δa being taken equal to a constant value (arbitrarily chosen) Fig. 9. In Fig. 9a, usually called "Iso curve" and which is the projection of the response surface on the plane, one can easily draw values predicted by the modeling other than those measured. The vertical analysis of Fig. 9b shows that for Δd equal to 0.07 mm, the accuracy error goes from 0.00512 for an Δα of −0.004° to 0.00201 for an Δα equal to 0.002°. Also, the accuracy error changes from a value of 0.0524 for Δα equal to −0.005 to an error of 0.00291 for Δd equal to 0.12 mm.

In Fig. 10 above, the value of Δa and the value of Δd are varied and the value of Δα of the robot is fixed. We then see that the precision error reaches a maximum with a value equal to approximately 0.0187 when Δa and Δd are equal

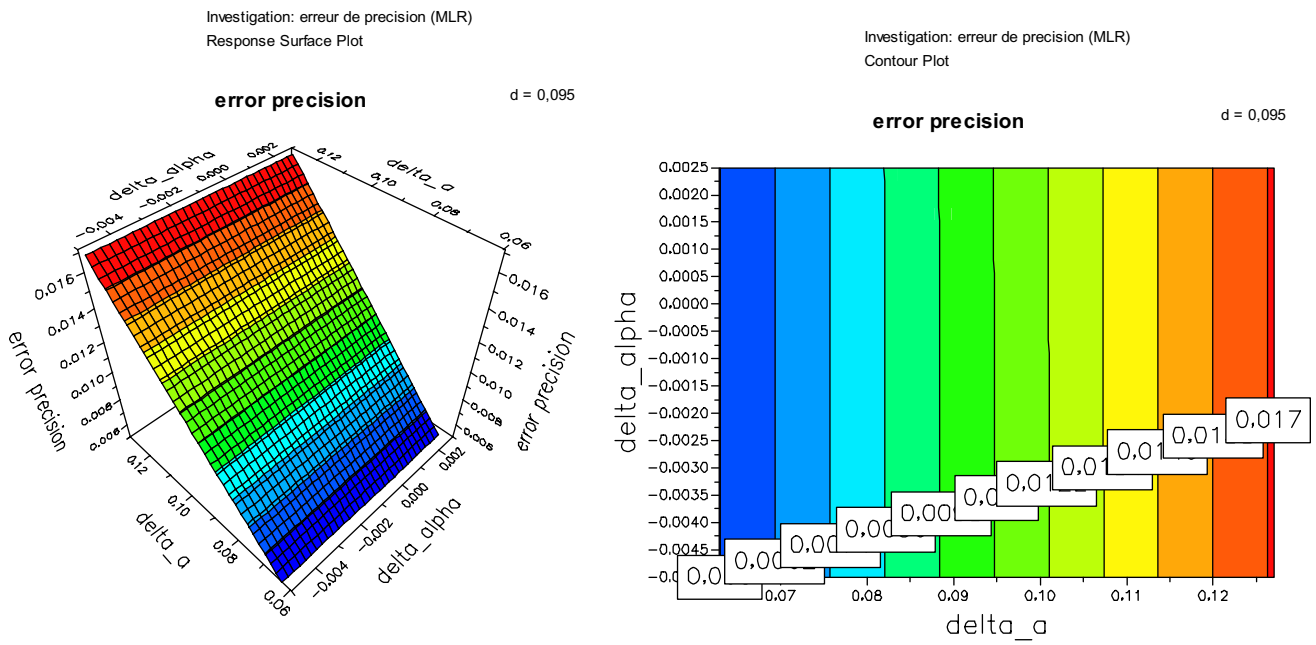

(a) Response surface with X1, X2 variables, X3 constant. **(b)** Interaction between X1and X2 fixed X3

Fig. 8 **a** Response surface with X1, X2 variables, X3. **b** Interaction between X1 and X2 fixed X3

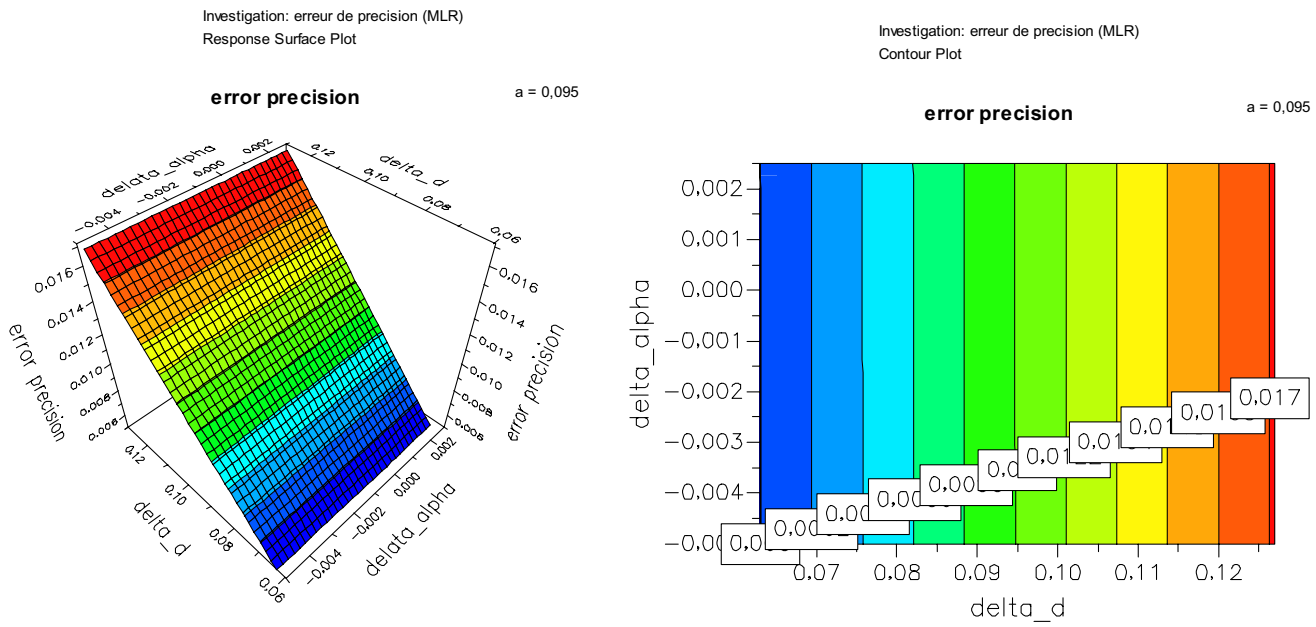

(a) Response surface with X1, X3 variables, X2 constant. **(b)** Interaction between X1and X3 fixed X2

Fig. 9 **a** Response surface with X1, X3 variables, X2 constant. **b** Interaction between X1 and X3 fixed X2

to 0.11 mm, this angle reaches 0.00902 for $\Delta a = 0.08$ mm and $\Delta d = 0.11$ mm. We also notice that this angle reaches an average value (between 0.00677 and 0.00584) if the Δd is fixed at its low level.

7.5 Variance estimation

The statistical calculations used to determine whether the effects are significant, to calculate the confidence

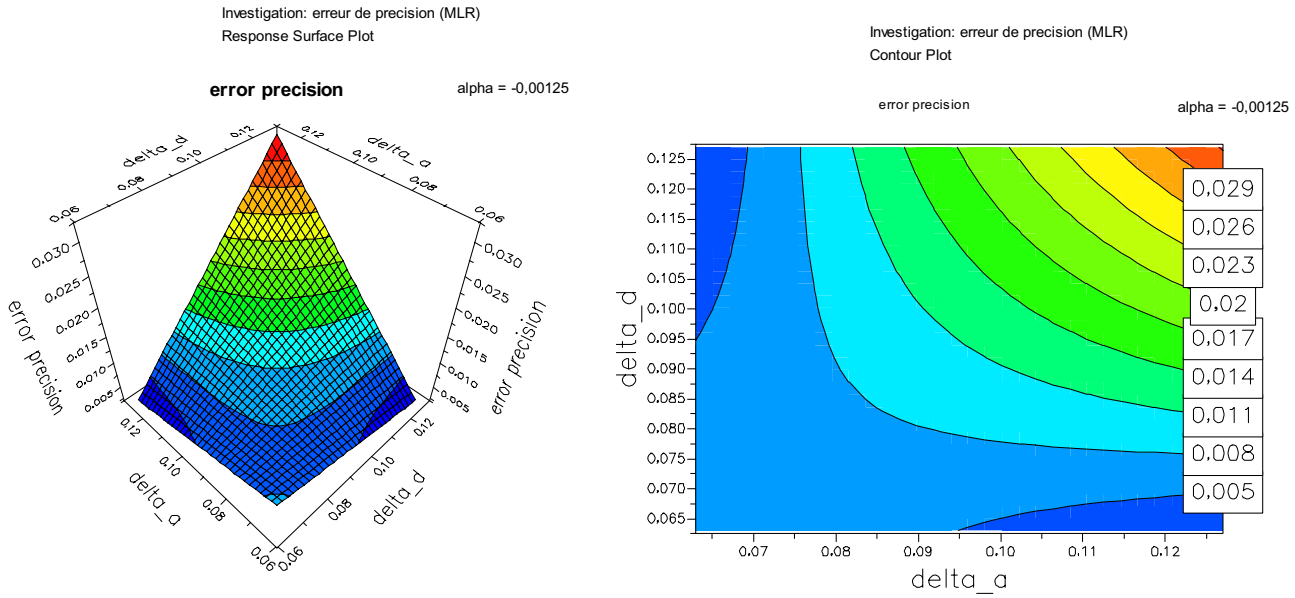

(a) Response surface with X3, X2 variables, X1 constant. **(b)** Interaction between X2and X3 fixed X1

Fig. 10 Response surface with X3, X2 variables, X1 constant. **b** Interaction between X2 and X3 fixed X_1

Table 8 Calculation of model residuals

Yestim	0,007938	0,007938	0,007938	0,007938	0,007938	0,007938	0,007938	0,007938
e_i	0,0	0,0	0,1e -8	0,1e -8	0,1e -8	0,1e -8	0,1e -8	0,1e -8

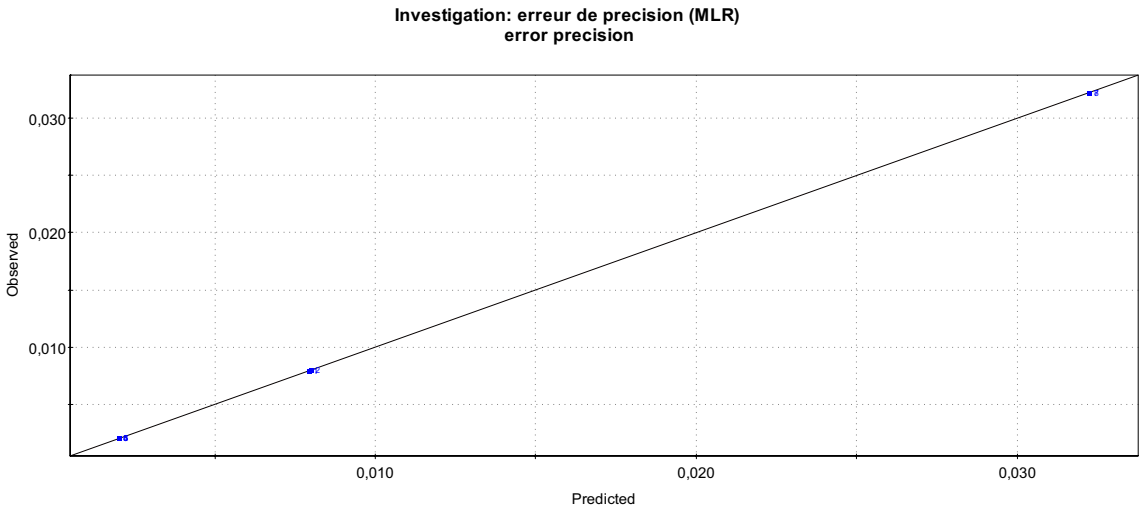

Fig. 11 Distribution of calculated responses with respect to the line

intervals and to validate the linearity of the model involve the residuals ei, i.e. the difference between the experimental value and the value predicted by the model (Tables 7 and 8).

7.6 Residue calculation

The absolute value of the difference between the experimental response and the predicted (estimated) response gives the value of the residual with relation (16):

$$e_i = \left| Y_{i\,\exp} - Y_{pre} \right| \tag{16}$$

These deviations show the difference between the experimental values and those described by the mathematical model. We find that they are insignificant and therefore we conclude that the model adequately describes the experimental. These deviations are visualized by (Fig. 11) in which we easily see a perfect correspondence between the linear model (right) and the tests.

7.7 Realization of the test of effects significance

The test used is Student's "t" test. An effect will be said to be significant (i.e. the variable or the interaction associated with it has an influence on the response), if it is, for a given risk, significantly different from 0.

We then use a Student's table with $\nu = n - p$ degrees of freedom (n is the number of experiments carried out and p the number of effects including the constant). We choose a risk of the first kind α (most often 5% or 1%) and the value tcrit(α, ν) is read from this Student table, using the part of the table relating to a bilateral test [20]. The test rule is then:

- If |the effect of a parameter |> tcrit(α, ν) * if: The effect is significant.
- If |the effect of a parameter |< tcrit(α, ν) *si: The effect is not significant.

The Student table gives for a risk α = 5% and v = n—p = 8—7 = 1,t_{crit}(0,05; 1) = 12,71.

An effect will therefore be significant at the 5% risk if it is "ti" and greater than 12.71. We get the following Table 9.

For this we use Student's test given by the relationship (17):

$$\mathbf{t}_i = |a_i| / S_i \tag{17}$$

8 Calculation of the variance

To further estimate the model, we first calculate the variance s, the square of which is expressed by:

$$S^2 = \frac{1}{n-p} \sum e_i^2 \tag{18}$$

$$s^2 = \frac{1}{8-7}(3{,}6e - 17)$$

Table 10 The confidence interval of model

	a_i	Upper limit	Lower limit
α_1	4,65661e-010	0.60350004	−0.603534
α_2	0,00608	0.609615	−0.59135
α_3	0,00608	0.609615	−0.59135
α_{13}	4,80682e-010	0.603535	−0.6035349
α_{23}	0,0090441	0.6125791	−0.5944909

Under these conditions, we can show that all effects have the same variance given by Eq. (19):

$$S_i^2 = \frac{S^2}{n} \tag{19}$$

where n is the number of experiments performed and p the number of model coefficients. Under these conditions, it can be shown that all the effects have the same variance given by:

$$\boldsymbol{S}_i^2 = \frac{3.6e-17}{8}$$

Consider our experimental design in which 2^3 neglecting the order of interaction 3, we collect residues and variances correspond to each effect in Table 5:

The common variance of residuals is given as follows:

$$S^2 = \frac{1}{n-p} \sum e_i^2 = \frac{1}{8-7}(0.01805) = 0.01805$$

The Student test table gives, for a risk of 5%with v = n − p (v dof) = 8–7 = 1 (dof)

$$t\,(\alpha;\nu) = t\,(0.05;\,1) = 12.71$$

One effect will be significant at the 5% risk if the "t_i" is greater than 12.71. Table 6 is obtained (Table 10).

We note that the effect of the interaction between the thickness and the yield strength (t_{12}) is not significant. Therefore, only the variables X_1, X_2, X_3 and I_{13} interactions, I_{23} are retained. And the model will become in the following form:

$$y = 0.0110539 + 0.00608X_2 + 0.00608X_3 + 0.0090441X_2X_3 \tag{20}$$

$$Ep = 0.0110539 + 0.00608a + 0.00608d + 0.0090441ad \tag{21}$$

Table 9 Significance of effects results

t_i	$t_0 = 164{,}781$	$t_1 = 0.06941$	$t_2 = 9063534.41$	$t_3 = 9063534.41$	$t_{12} = 0.07165$	$t_{13} = 0.03134$	$t_{23} = 1348215.61$
Results	Significant	Not significant	Significant	Significant	Not significant	Not significant	Significant

8.1 The confidence interval of model

We will find a confidence interval at the risk of 5%, for the significant effects: a1, a2, a3, a12 and a13, If we choose a risk α we can determine the value of t (α; v) using the Student table and the confidence interval of an effect is given by:

$$\text{Risk } \alpha_i : \left[(a_i - t(\alpha, v)S_i; \left(a_i + t(\alpha, v)S_i\right)\right] \quad (22)$$

After replacing the values of t(α; v) and S i we obtain:

$$\alpha_i = \left[a_i - 12.706 * 0,0475; a_i + 12.706 * 0.0475\right]$$

$$\alpha i : [(ai - t(\alpha, v)Si; (ai + t(\alpha, v)Si]$$

Table 7 shows the confidence interval of significant effects coefficients:

9 Conclusion

The work presented was devoted to the study of improving the precision and repeatability of a robotic system. For example, improving the manufacturing quality of robot components helps reduce tolerances and thus limit geometric errors. Robot calibration is the solution that improves the static precision of robot positioning without any modification of the structure. Our work is devoted to geometric calibration. The work consists in analyzing the static errors of precision and repeatability of a robotic system given by these DH parameters (standard or modified), knowing the precision on each link (Δq, Δα, Δd), and in calculating the overall systematic precision. From the choice of an initial pose (zero position), the global error is analytically evaluated.

We were then interested in the simulation of the precision and repeatability of the first link or link of the puma 560 robot. This part allowed us to draw the following conclusions:

- The evolution of the various parameters governing the precision error converges in the same direction;
- The higher the tolerance on the geometric parameters (Δa, Δd), the greater the precision error.
- To improve precision, we must reduce the geometric tolerance on the first links (on machining).

Subsequently, we studied by the method of design of experiments the effect of the static errors of each parameter of the first link (predominant effect) of the puma 560 robot on the precision of the robots. The following results:

- The precision error increases with increasing tolerances of the geometric parameters (Δa, Δd);
- The most significant influence of these parameters on the overall error.
- The influence of the angle (Δα) has an insignificant effect on the precision of the robot To calibrate a robot, it is necessary to intervene on the first link.

Acknowledgements This work has been carried out at the Laboratory of Structures and Solids Mechanics. Extend my sincere thanks to all members participating in the preparation of this work.

Declarations

Conflict of interest The authors declare that they have no conflict of interest.

Ethical approval This content of this paper has been prepared in compliance with the ethics rules of the authors' home institutions and Springer.

Consent for publication Not applicable.

Data availability Not applicable.

References

1. Young K, Pickin CG (2000) Accuracy assessment of the modern industrial robot. Ind Robot Int J 27:427–436
2. John JC (1989) Introduction to ROBOTICS-mechanics and control, 2nd Edn
3. Kadem M, Semmah A, Wira P et al (2020) Artificial Neural Network active power filter with immunity in distributed generation. Period Polytech Mech Eng 64(2):109–119
4. Slimane SA, Slimane A, Guelailia A et al (2021) Hypervelocity impact on honeycomb structure reinforced with bi-layer ceramic/aluminum facesheets used for spacecraft shielding. Mech Adv Mater Struct 29:4487–4505
5. Dumas C, Boudelier A, Caro S et al (2011) Développement d'une cellule robotisée de détourage des composites. Mech Ind 12(6):487–494
6. Roth ZVIS, Mooring B, Ravani B (1987) An overview of robot calibration. IEEE J Robot Automat 3(5):377–385
7. Dahmane S-A, Azzedine A, Megueni A et al (2019) Quantitative and qualitative study of methods for solving the kinematic problem of a planar parallel manipulator based on precision error optimization. Int J Interact Des Manuf (IJIDeM) 13(2):567–595
8. Gong C, Yuan J (2000) Ni J (2000) Nongeometric error identification and compensation for robotic system by inverse calibration. Int J Mach Tools Manuf 40(14):2119–2137
9. Nehari L, Brahami M, Slimane A (2019) Integrating a new adaptive PV system for ozone production process. Electr Eng 101(2):647–657
10. Slimane S, Kebdani S, Boudjemai A et al (2018) Effect of position of tension-loaded inserts on honeycomb panels used for space applications. Int J Interact Des Manuf (IJIDeM) 12(2):393–408
11. Hollerbach JM, Wampler CW (1996) The calibration index and taxonomy for robot kinematic calibration methods. Int J Robot Res 15(6):573–591

12. Dahmane SA, Azzedine A, Megueni A (2020) Ant colony optimization algorithm based on optimal PID parameters for a robotic arm. Int J Control Syst Robot 5:8–13
13. Quinet JF (1995) Calibration for offline programming purpose and its expectations. Ind Robot Int J 22:9–14
14. Bahram K, Chaib M, Slimene A et al (2020) Simulation of the delay effect after applying a simple overload on alloys of aluminum 2024T351 using the Willemborg model. Frattura ed Integrità Strutturale 14(51):467–476. https://doi.org/10.3221/IGF-ESIS.51.35
15. Kaddour B, Bouchouicha B, Benguediab M et al (2018) Modeling and optimization of a cracked pipeline under pressure by an interactive method: design of experiments. Int J Interact Des Manuf (IJIDeM) 12(2):409–419
16. Janocha H, Diewald B et al. (1995) ICAROS: over-all-calibration of industrial robots. Ind Robot Int J
17. Denavit J, Hartenberg RS (1955) A kinematic notation for lower-pair mechanisms based on matrices
18. Dahmane SA, Megueni A, Azzedine A et al (2019) Determination of the optimal path of three axes robot using genetic algorithm. Int J Eng Res Afr 44:135–149
19. Alban T, Janocha H (1999) Dynamic calibration of industrial robots with inertial measurement systems. In: 1999 European control conference (ECC). IEEE, 1999. p. 785-790
20. Shiakolas PS, Conrad KL, Yih TC et al (2002) On the accuracy, repeatability, and degree of influence of kinematics parameters for industrial robots. Int J Model Simul 22(4):245–254
21. Rocadas PS, Mcmaster RS (1997) A robot cell calibration algorithm and its use with a 3D measuring system. In: ISIE'97 proceeding of the IEEE international symposium on industrial electronics. IEEE, 1997. p. SS297-SS302
22. Slimane A, Bouchouicha B, Benguediab M et al (2015) Parametric study of the ductile damage by the Gurson–Tvergaard–Needleman model of structures in carbon steel A48-AP. J Market Res 4(2):217–223
23. Nagesh DS, Datta GL (2008) Modeling of fillet welded joint of GMAW process: integrated approach using DOE, ANN and GA. Int J Interact Des Manuf (IJIDeM) 2(3):127–136
24. Slimane A, Bouchouicha B, Benguediab M et al (2015) Contribution to the study of fatigue and rupture of welded structures in carbon steel-a48 ap: experimental and numerical study. Trans Indian Inst Met 68(3):465–477
25. Slimane A, Kebdani S, Bouchouicha B et al (2018) An interactive method for predicting industrial equipment defects. Int J Adv Manuf Technol 95:4341–4351
26. Valinejad R, Nazar ARS (2013) An experimental design approach for investigating the effects of operating factors on the wax deposition in pipelines. Fuel 106:843–850
27. Slimane A, Slimane S, Kebdani S et al (2019) Parameters effects analysis of rotary ultrasonic machining on carbon fiber reinforced plastic (CFRP) composite using an interactive RSM Method. Int J Interact Des Manuf (IJIDeM) 13(2):521–529
28. Chaib M, Slimane A, Slimane SA et al (2021) Optimization of ultimate tensile strength with DOE approach for application FSW process in the aluminum alloys AA6061-T651 & AA7075-T651. Frattura ed Integrità Strutturale 15(57):169–181
29. Nagesh DS (2008) Datta GL Modeling of fillet welded joint of GMAW process: integrated approach using DOE, ANN and GA. Int J Interact Des Manuf (IJIDeM) 2(3):127–136
30. Moghaddam AS, Mohammadnia S, Sagharichiha M (2015) Analysis of offshore pipeline laid on 3D seabed configuration by Abaqus. Ocean Syst Eng 5(1):31–40
31. Chatterjee AN, Kumar S, Saha P et al (2003) An experimental design approach to selective laser sintering of low carbon steel. J Mater Process Technol 136(1–3):151–157
32. Ilzarbe L, Alvarez MJ, Viles E et al (2008) Practical applications of design of experiments in the field of engineering: a bibliographical review. Qual Reliab Eng Int 24(4):417–428